Research Article

Structural, Optical, Antibacterial and Anticancer Properties Silver Barium Modified Titanium Dioxide Nanoparticles Prepared via a Green Process Using *Withania somnifera* Hairy Roots

Raja Palusamy[1], Thiagu Ganesan[1], Appakan Shajahan[1,*], Thilip Chandrasekaran[2], Alagar yadav Sangilimuthu[3], Liyahathalikhan Umaralikhan[4]

[1]Department of Botany, Plant Molecular Biology Laboratory, Jamal Mohamed College (Autonomous), Affiliated to Bharathidasan University, Tiruchirappalli, Tamil Nadu, INDIA.
[2]Department of Botany, Government Arts and Science College, Sendamangalam, Namakkal, Tamil Nadu, INDIA.
[3]Department of Biotechnology, Karpagam Academy of Higher Education, Coimbatore, Tamil Nadu, INDIA.
[4]Department of Physics, Jamal Mohamed College (Autonomous), Affiliated to Bharathidasan University, Tiruchirappalli, Tamil Nadu, INDIA.

Submission Date: 27-06-2023; Revision Date: 14-08-2023; Accepted Date: 22-09-2023.

ABSTRACT

Aims: The current study sought to assess the antibacterial and anticancer properties of AgBa-modified TiO_2 nanoparticles produced by a green method using a hairy root extract from *Withania somnifera*. **Materials and Methods:** The synthesized samples were examined through X-ray Diffraction (XRD) investigations, SEM and Energy-Dispersive X-ray analysis (EDX), Dynamic Light Scattering (DLS), Fourier Transform Infrared (FTIR) Spectroscopy, Ultraviolet (UV) Spectroscopy, and Photoluminescence (PL) spectra. **Results:** SEM validated the produced nanoparticle's spherical-like shapes with EDX analysis, which confirmed the crystallite size of 70 nm as determined by DLS. In addition, oxygen vacancies in synthesized nanoparticles were found between 501 and 521 nm in the PL spectra. **Conclusion:** The primary focus of this study is on the environmentally friendly plant-based synthesis of biomedically important AgBa-modified TiO_2 using aqueous *Withania somnifera* hairy root, and it has the potential antibacterial against *S. aureus*, *S. pneumoniae*, *B. subtilis, K. pneumoniae, E. coli, P. vulgaris* and anticancer activity against blood cancer cell lines (MOLT-4).

Keywords: AgBa modified TiO_2, Green process, *Withania somnifera* hairy roots, Antibacterial, Anticancer activity.

Correspondence:
Dr. Appakan Shajahan,
PG and Research, Department of Botany, Plant Molecular Biology Laboratory, Jamal Mohamed College (Autonomous), Tiruchirappalli-620 020, Tamil Nadu, INDIA.

Email: shajahan.jmc@gmail.com, rajams116@gmail.com

INTRODUCTION

A current hotbed of materials science research is nanotechnology. Innovative fabrics, food processing, crop growth, and cutting-edge medical procedures are just a few examples of the new things that this technology can make possible.[1] It involves developing, identifying, and studying materials with a nanometer-sized size range (1-100 nm). Nanoparticles (NPs) have a larger surface area than macroparticles because they are smaller in size.[2] They differ significantly from bulk materials in terms of their size-dependent properties.[3] Despite being smaller than their counterparts, NPs have more substantial structures. Because of this particular property, they could be utilized in various applications, such as biosensors, nanomedicine, and bionanotechnology.[2-6] Metal NPs TiO_2's size, makeup, degree of crystallinity, and shape reveal a lot about their innate characteristics.

When materials are scaled down to the nanoscale, their chemical, mechanical, electrical, structural,

SCAN QR CODE TO VIEW ONLINE

www.ajbls.com

DOI: 10.5530/ajbls.2023.12.40

morphological, and optical properties can change. Nanomaterials have consequently recently been given a lot of attention in both the basic and applied sciences, as well as in bionanotechnology.

Many researchers have investigated the nano-sized $BaTiO_3$, which has a variety of morphologies and demonstrates significant antibacterial and anticancer properties. $BaTiO_3$ is currently being researched as a potential antibacterial ingredient in nano- and microscale formulations. When BaTiO3 particles are sized to the nanometer range, they exhibit strong antimicrobial properties.

Once inside the bacterial cell, BaTiO3 interacts with the surface of the core of the bacteria and then indicates specific bactericidal mechanisms.[7-9]

As part of the synthesis process, various parameters are subjected to optimization and control to obtain $BaTiO_3$ nanomaterials, even though biological substances offer an alternative to green chemistry for producing nanoparticles that are harmless to humans and the environment.[5,10] Using green synthesis methodology, we used the extract of *W. somnifera* hairy roots acting as a reducing and capping agent while preparing a novel kind of $BaTiO_3$:Ag nanoparticles. This was done to produce potential antimicrobial nanocomposites.

In several countries, *W.somnifera* roots are used as essential ethnomedicinal herbs. In some countries like Morocco, South Africa, Tanzania, India, Ethiopia, Lesotho, and Pakistan, the WSR extract was used for curing the following diseases Abortifacients, Sedatives, Aphrodisiacs, Kidneys, Fever, Ethnoveterinary, Gynaecological, and Pulmonary troubles.[11] The main objective of this study is to investigate the structural and optical properties of Green synthesized AgBa-modified TiO_2 (GABT) using WSR. Furthermore, the antibacterial and anticancer activity of synthesized GABT was also analyzed.

MATERIALS AND METHODS

Materials

Barium nitrate (98%), Silver nitrate and titanium isopropoxide were purchased from Sigma Aldrich.

Preparation of natural *Withania somnifera* hairy roots (WSR) reduction agent

The 5 g of dried *W. somnifera* hairy roots (WSR) powder was mixed with 100 mL of deionized water. The *W. somnifera* hairy roots (WSR) solution was boiled at 80°C for 20 min on a magnetic stirrer. After that, the *Amomum subulatum* Roxb solution mixture was filtered using Whatman No. 1 paper. Filter WSR solution stored in the refrigerator.

Green synthesis of AgBa-modified TiO_2

To prepare AgBa-modified TiO_2 (GABT) NPs, 0.005 M of barium nitrate and 0.005 M of silver nitrate solute were added to 0.090 M of titanium isopropoxide solution. Next, the Ti metal solution was added to 100 mL of WSR extract to produce a white, homogenous solution. This titanium precipitate solution was stirred continuously at 80°C for 4-6 hr. The precipitate was then calcined at 700°C for 5 hr.

Characterization techniques

The GABT NPs were characterized by an X-ray diffractometer (model: X'PERT PRO PANalytical). The diffraction patterns were recorded in the 20°–80° for the GABT NPs, where the monochromatic wavelength of 1.54 was used. The samples were analyzed by field emission scanning electron microscopy (Carl Zeiss Ultra 55 FESEM) with EDAX (model: Inca). The NanoPlus Dynamic Light Scattering (DLS) Nano Particle Sizer was used for the particle size analysis of the GABT NPs. The FTIR spectrum was recorded in the wavenumber range of 400–4000 cm^{-1} by using the Perkin-Elmer spectrometer. The UV-vis NIR spectrum was captured using Lambda 35 at wavelengths ranging from 200 to 1100 nm. Photoluminescence spectra were measured using the Cary Eclipse spectrometer.

Antibacterial assay

The antibacterial activity of the above GABT nanoparticles was investigated by the well diffusion method and tested against G+ (*S. aureus, S. pneumoniae* and *B. subtilis*) G-bacteria (*K. pneumoniae, E. coli* and *P. vulgaris*) after molten nutrient agar, according to the Clinical and Laboratory Standards Institute (CLSI). After inoculation, well loaded with 1, 1.5, and 2 mg/mL of the test samples were placed on the bacteria-seeded well plates using micropipettes. The plates were then incubated at 37°C for 24 hr. The inhibition zone was measured. As a positive control for G+ and G-bacteria, amoxicillin (Hi-Media) was used.

Cell culture maintenance

Blood cancer cell (MOLT-4) lines were procured from the cell repository of the National Centre for Cell Sciences (NCCS), Pune, India. Dulbecco's Modified Eagle Media (DMEM) was used for maintaining the cell line, which was supplemented with 10% Fetal Bovine Serum (FBS). Penicillin (100 U/mL), and streptomycin (100 µg/mL) were added to the medium to prevent bacterial contamination. The medium with cell lines

was maintained in a humidified environment with 5% CO_2 at 37°C.

MTT stock solution

MTT (50 mg) dye was dissolved in 10 mL of PBS. After vertexing for 1 min, it was filtered through 0.45 micro filters. The bottle was wrapped with aluminium foil to prevent light, as MTT was light-sensitive. The preparation was stored at 4°C.

MTT assay

Cell viability assay, Blood cancer cell (MOLT-4) cells were harvested and counted using a haemocytometer diluted in DMEM medium to a density of 1×10^4 cells/mL was seeded in 96 well plates for each well and incubated for 24 hr to allow attachment. After Blood cancer cell (MOLT-4) cells were treated with control and the containing different concentrations of sample GABT NPs at 5 to 20 µg/mL were applied to each well. Blood cancer cell (MOLT-4) cells were incubated at 37°C in a humidified 95% air and 5% CO_2 incubator for 24 hr.

After incubation, the drug-containing cells were washed with fresh culture medium and the MTT (5 mg/mL in PBS) dye was added to each well, followed by incubation for another 4 hr at 37°C. The purple precipitated formazan formed was dissolved in 100 µL of concentrated DMSO and the cell viability was absorbance and measured 540 nm using a multi-well plate reader. The results were expressed at the percentage of stable cells with respect to the control.

The half-maximal inhibitory concentration (IC_{50}) values were calculated, and the optimum doses were analysed at different time.

$$\text{Cell viability (\%)} = \frac{\text{Mean absorbance of the control} - \text{Mean absorbance of the sample}}{\text{Mean absorbence of the control}} \times 100$$

The IC_{50} values were determined from the sample A and B dose-responsive curves where inhibition of 50% cytotoxicity compared to vehicle control cells. All experiments were performed at least three times in triplicate.

RESULTS AND DISCUSSION

Figure 1 shows the XRD pattern of the GABT. The perovskite phase with a rutile TiO_2 structure (JCPDs No. 75-1537) is correspondingly represented by the diffraction peaks in the GABT sample, which can be found at angles (2θ) of 24.91, 30.19, 37.15, 43.82, 54.39, and 64.26. These angles correspond to the (001), (110), (111), (200), (211), and (220) hkl PLANE.[12] In addition, secondary phases were indexed to the tetragonal phase of BaO and were in good agreement with JCPDS Card No. 26-0178".[13] The anatase phase structure of TiO_2 was also in good agreement with JCPDS card No. 21-1272,[14] and peaks of Ag were found to be in good agreement with JCPDS card No. 04-0783.[15] Peaks that are both sharp and intense are evidence that the nanoparticles synthesized are highly crystalline in their natural state. The average crystallite size (D) of the sample is determined by applying the formula developed by Debye and Scherrer, which can be written as follows:

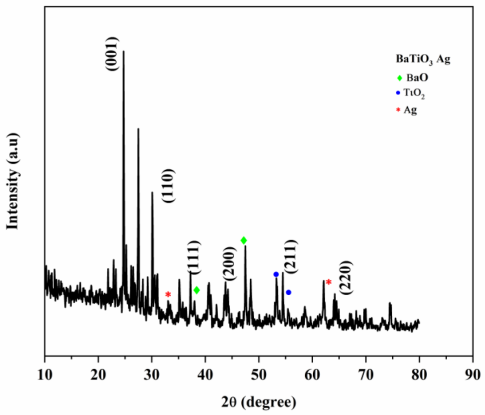

Figure 1: XRD pattern of the GABT.

$$D = \frac{k \cdot \lambda}{\beta \cdot \cos\theta} \quad (1)$$

Here, the Size of the nanoparticles is named "D", radiations wavelength is named as "λ", a constant 0.94 is named as "*k*", the peak width at half-maximum intensitynamed as "*β*", peak position named as "*θ*". The average crystallite size is 55.1 nm.

Dynamics light scattering studies

The Dynamic Light Scattering (DLS) method is a technique for analyzing particle size and size distribution. The particle size distribution of GABT nanoparticles was diagnosed with the help of this technique. Figure 2 illustrates that 50% of the particles had a size of up to 70 nanometers, while the other 50% were more significant.

SEM and EDAX spectral analysis

Figure 3a displays scanning electron micrographs that were taken of synthesized GABT. The structure resembles a brain coral, with some spherical-like structures scattered throughout. Figure 3a shows the spherical structure of AgBa nanoparticles that are

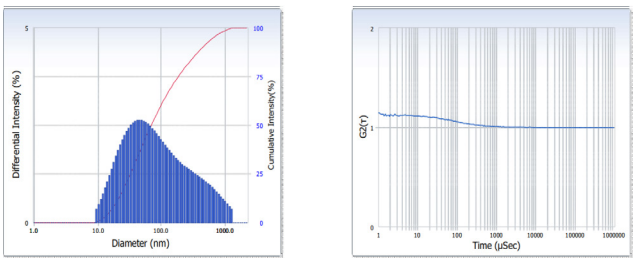

Figure 2: DLS analysis of GABT.

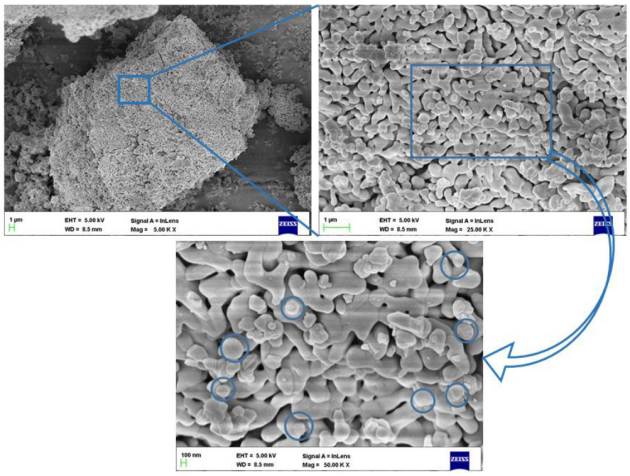

Figure 3: a. SEM image of GABT.

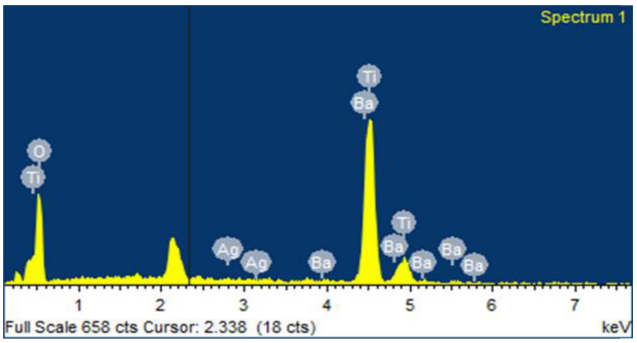

Figure 3: b. EDAX spectral image of GABT.

attached to the TiO_2 brain coral structure. The results of the EDX analysis, which can be seen in Figure 3b, confirmed the presence of the elements Ba, Ti, Ag, and O in the GABT nanoparticles that had been synthesized. We could determine the composition of this sample by examining it in three different locations. They have comparable values (within 0.01 at. %), indicating that the sample composition is uniform throughout. Ba, Ti, Ag, and O account for 24,44%, 43.10%, 11.28%, and 21,21% of the total elemental atomic composition.

FTIR spectral analysis

We perform FTIR spectroscopy in the range of 4000-400 cm^{-1} to classify the functional groups present

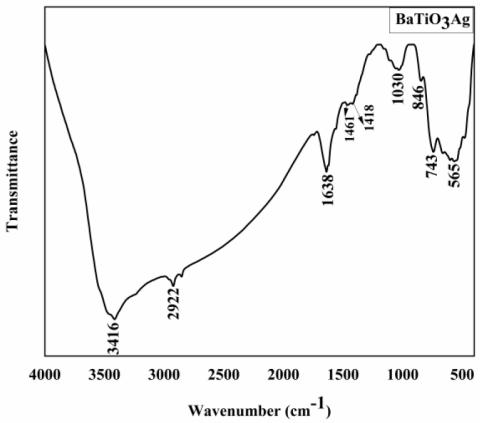

Figure 4: FTIR spectroscopy of GABT.

in the aqueous extract and the zinc oxide nanoparticles, as shown in Figure 4. These functional groups are present in both of these samples. We did this so that we could evaluate the outcomes side by side. The small peaks at 846 cm^{-1} represent Ag-O,[16] 743 and 565 cm^{-1} represent Ti-O stretching bands[17] of the GABT. The peaks that appear between 1418 and 1461 cm^{-1} are associated with the stretching vibration of C–O–CO_3^{2-} caused by traces of $BaCO_3$. It is evident from Figure 3 that the hydroxy functional group is present due to the decrease in intensity of the peak corresponding to –OH groups at 3416 cm^{-1}. A peak at 1638 cm^{-1}, characteristic of the bending mode of H–O–H, is the result of water being physically adsorbed on $BaTiO_3$ nanoparticles. It was determined that the band with a frequency of 2922 cm^{-1} was the stretching vibration of C–H bands associated with propyl groups[18] of WSR.[19]

UV–vis absorbance spectra analysis

The UV–vis absorbance spectra were utilized to investigate the GABT's optical characteristics. The band gap, the amount of oxygen deficiency, the number of impurity centres, the roughness of the surface, the impurity centres, and the quantum confinement effect were all factors that determined the absorbance of the samples.[20] Because of the reduction in particle size, one can anticipate the occurrence of quantum confinement effects.

These effects will be noticeable as a blue shift of the optical absorption edge, which is brought about by widening the band gap in the ultraviolet region. The absorption spectrum (Figure 5). displays a blue shift at 397 nm, associated with the bulk exciton. This particular property is of the utmost importance to the quantum confinement effect in GABT nanostructured materials.

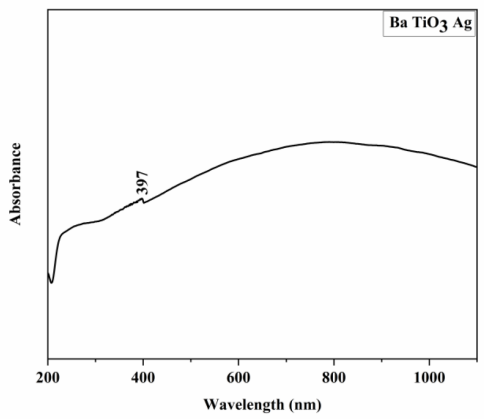

Figure 5: UV spectra of GABT.

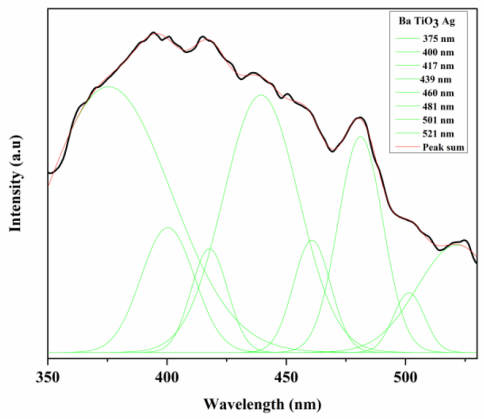

Figure 6: PL spectra of GABT.

In addition, it was discovered that the GABT sample had an energy band gap of 3.12 eV.

PL analysis

Photoluminescence of GABT at room temperature is reported in Figure 6. The deconvolution in eight distinct bands, where the first maximum occurred at around 3.31 eV, followed by a maximum at 3.10 eV, 2.97 eV, 2.82 eV, 2.70 eV, 2.58eV, 2.47 eV, and one at 2.38 eV. The PL spectra of GABT depicted in the figure are composed of three colour components, the violet emission at 375 nm with 3.31eV equivalent to the typical band gap of BaTiO3, near band emission at 400 nm with 3.10 eV, 417 nm with 2.97 eV. The blue emission peaks at 439 nm with 2.82 eV, 460 nm with 2.70 eV, and 481 nm with 2.58 eV, which represents, that there must exist certain localized levels within the forbidden band gap because the direct electron transition between the valence band and the conduction band should not be allowed.[21,22]

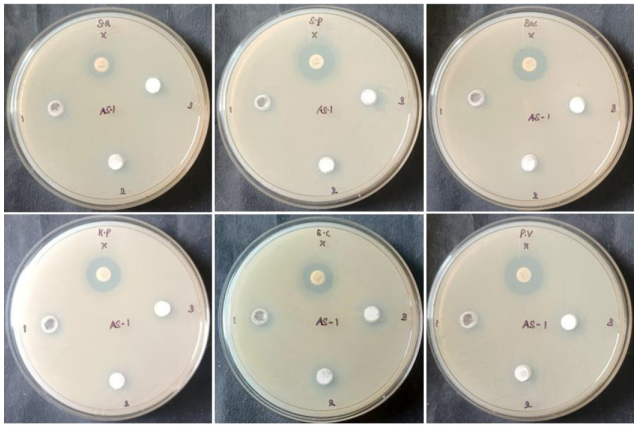

Figure 7: Antibacterial activity of GABT NPs treated with *S. aureus*, *S. pneumoniae*, *B. subtilis*, *K. pneumoniae*, *E. coli*, and *P. vulgaris* bacterial strain.

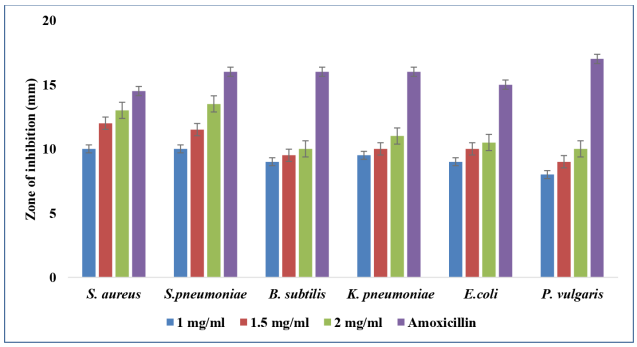

Figure 8: Zone of inhibition of GABT NPs treated with *S. aureus*, *S. pneumoniae*, *B. subtilis*, *K. pneumoniae*, *E. coli*, and *P. vulgaris* bacterial strain.

The green emission at 501 nm with 2.47 eV and 521 nm with 2.38 eV provides evidence that the latter encountered improved charge separation and demonstrated a decreased recombination rate. These effects would increase the probability that electrons and holes will combine to form reactive oxygen species ROS, increasing photocatalytic activity.[23]

Antibacterial activity

The well diffusion method was used to assess Figure 7. antibacterial activity of GABT NPs against *S. aureus, S. pneumoniae, B. subtilis, K. pneumoniae, E. coli,* and *P. vulgaris*. The results are presented in Figure 8. As depicted in Figure 9, the Zone of Inhibition of GABT NPs and conventional medicines like amoxicillin exhibit antibacterial activity. Therefore, the concentration and antibacterial activity of GABT NPs should be increased. Compared to other gram-positive and gram-negative bacterial cultures, *B. subtilis* demonstrates the highest inhibition rate, demonstrating how effective synthetic GABT NPs are against all bacterial pathogens. XRD measurements determine the GABT particle size

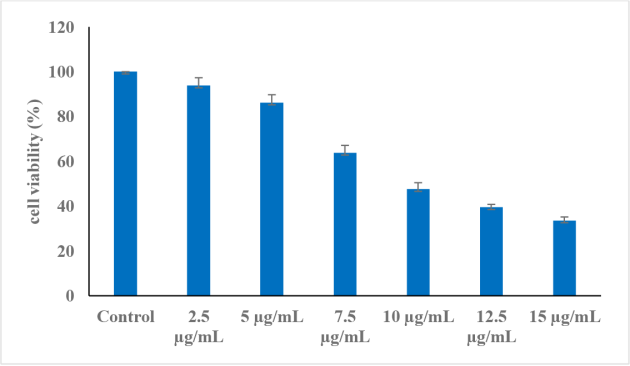

Figure 9: Anticancer activity of GABT NPs treated with Blood cancer MOLT-4 cells for 24 hr.

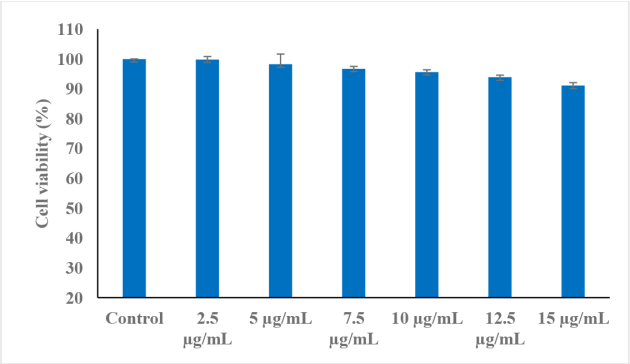

Figure 10: Toxicity activity of GABT NPs treated with Blood cancer MOLT-4 cells for 24 hr.

in the current study to be around 55 nm, and the surface defect (Oxygen vacancies: Ov) of the GABT is shown by the PL spectra at 501 and 521 nm. If a nanomaterial exhibits essential photocatalytic activity and oxygen vacancies, it frequently produces more ROS. In this illustration, water splitting within the cell's cytoplasm may produce active free radicals such as singlet oxygen and hydroxide radicals. Bacterial cells contain DNA and lipid macromolecules that interact with single oxygen and hydroxide radicals, or ROS, to disturb the physiological processes going on inside the cell.

Anticancer activity

The anticancer activity of AgBa-modified TiO_2 NPS was tested on the viability of human blood cancer cell MOLT-4 cells at various concentrations ranging from 2.5 to 15 g/mL at 37ºC for 24 hr. After incubation, cytotoxicity was tested using the MTT assay. Figure 9 show the MOLT-4 cell lines treated with GABT NPs demonstrated anticancer activity at all concentrations tested (2.5 to 15 g/mL). In addition, due to the cytotoxic inhibition activity of Reactive Oxygen Species (ROS)-induced cell death, the IC_{50} estimates of cell inhibition of GABT NPs were observed to be 9.5 g/mL.

In vitro toxicity

GABT's cytotoxicity was tested on L929 cells. An optical microscope determined whether L929 cells had undergone any morphological changes, as shown in Figure 10. A homogeneous fusiform shape can be seen in the untreated control cell (100% cell viability). The manufactured GABT-treated cells showed 91% vitality, indicating that they were still alive.

CONCLUSION AND SUMMARY

The primary focus of this study is on the environmentally friendly plant-based synthesis of biomedically important AgBa-modified TiO_2 using aqueous WRS, an essential plant in conventional medicine. Using XRD analysis, the crystalline structure of the generated GABT NPs was determined to be a tetragonal structure. The morphologies and elemental content of synthesized GABT were determined using FSEM and EDX. The presence and concentration of Ba, Ti, Ag, and O account for 24.44%, 43.10%, 11.28%, and 21.21% were confirmed by EDX spectra. Particle sizes as small as 70 nm are revealed by DLS analysis. The phytochemicals in the WRS in the sample were confirmed by FTIR spectroscopy analysis. At 848 and 1461 cm^{-1}, the WRS (COO-) acid ligand was discovered. It demonstrates that synthetic GABT still contains plant-based precursors. The primary electron transition between inter-bands and direct bands was visible in the PL spectra, along with trap-state emission. The synthesized GABT NPs can kill both G+ and G-type bacterial strains. The anticancer activity of GABT NPs against blood cancer cell lines increased as their concentration increased.

ACKNOWLEDGEMENT

The authors express their heartful thanks to Dr. A. Shajahan and DST, Govt. of India for providing facilities through the DST-FIST Program and DBT, Govt. of India for their support through Star College scheme.

CONFLICT OF INTEREST

The authors declare that there is no conflict of interest.

Author's contributions

Appakan Shajahan: Conceived the topic and designed the study. **Palusamy Raja:** Data curation, investigation, methodology, writing the original draft. **Ganesan Thiagu:** Field work and lab assistance. **Chandrasekaran Thilip:** Workflow and instrumentation. **Alagar yadav Sangilimuthu:** Workflow and instrumentation.

Liyahathalikhan Umaralikhan: Writing and review and editing.

Availability of data and materials

All datasets generated or analysed during this study are included in the manuscript.

ABBREVIATIONS

WSR: *Withania Somnifera* Roots; **AgBa:** Silver Barium; **TiO_2:** Titanium Dioxide; **XRD:** X-ray Diffraction; **SEM:** Scanning Electron Microscope; **EDX:** Energy-Dispersive X-ray analysis; **DLS:** Dynamic Light Scattering; **FTIR:** Fourier Transform Infrared Spectroscopy; **UV:** UltraViolet; **PL:** Photo Luminescence; **NPs:** Nanoparticles; **ROS:** Reactive Oxygen Species; **MTT:** 3-(4,5-dimethylthiazol-2-yl)-2,5-diphenyl-2H-tetrazolium bromide; **IC_{50}**: Half-maximal inhibitory concentration; **DMEM:** Dulbecco's Modified Eagle Medium; **PBS:** Phosphate buffered saline.

REFERENCES

1. Sahoo S. Socio-ethical issues and nanotechnology development: perspectives from India. In10th IEEE international conference on nanotechnology. IEEE Publications. 2010:1205-10. doi: 10.1109/NANO.2010.5697887.
2. Ashe B. A Detail investigation to observe the effect of zinc oxide and silver nanoparticles in biological system [doctoral dissertation].
3. Buzea C, Pacheco II, Robbie K, Robbie K. Nanomaterials and nanoparticles: sources and toxicity. Biointerphases. 2007;2(4):MR17-71. doi: 10.1116/1.2815690, PMID 20419892.
4. Karthikeyan C, Sisubalan N, Varaprasad K, Aepuru R, Yallapu MM, Viswanathan MR, *et al*. Hybrid nanoparticles from chitosan and nickel for enhanced biocidal activities. New J Chem. 2022;46(27):13240-8. doi: 10.1039/D2NJ02009B.
5. Umaralikhan L, Jamal Mohamed Jaffar M. M. Green synthesis of MgO nanoparticles and it antibacterial activity. Iran J Sci Technol Trans A Sci. 2018;42(2):477-85. doi: 10.1007/s40995-016-0041-8.
6. Umaralikhan L, Jaffar MJ. Antibacterial and anticancer properties of NiO nanoparticles by co-precipitation method. J Adv Appl Sci Res 2016;1(4):24-35. doi: 10.46947/joaasr14201628.
7. Shah AA, Khan A, Dwivedi S, Musarrat J, Azam A. Antibacterial and antibiofilm activity of barium titanate nanoparticles. Mater Lett 2018;229:130-3. doi: 10.1016/j.matlet.2018.06.107.
8. Ahamed M, Akhtar MJ, Khan MAM, Alhadlaq HA, Alshamsan A. Barium titanate (BaTiO3) nanoparticles exert cytotoxicity through oxidative stress in human lung carcinoma (A549) Cells. Nanomaterials (Basel). 2020;10(11). doi: 10.3390/nano10112309, PMID 33266501.
9. Fakhar-e-Alam M, Saddique S, Hossain N, Shahzad A, Ullah I, Sohail A, *et al*. Synthesis, characterization, and application of BaTiO3 nanoparticles for anti-cancer activity. J Clust Sci. 2023;34(4):1745-55. doi: 10.1007/s10876-022-02346-y.
10. Umaralikhan L, Jaffar MJM. Green synthesis of ZnO and Mg doped ZnO nanoparticles, and its optical properties. J Mater Sci Mater Electron. 2017;28(11):7677-85. doi: 10.1007/s10854-017-6461-1.
11. Afewerky HK, Ayodeji AE, Tiamiyu BB, Orege JI, Okeke ES, Oyejobi AO, *et al*. Critical review of the *Withania somnifera* (L.) Dunal: ethnobotany, pharmacological efficacy, and commercialization significance in Africa. Bull Natl Res Cent. 2021;45(1):176. doi: 10.1186/s42269-021-00635-6, PMID 34697529.
12. Khan TM, Zakria M, Shakoor RI, Hussain S. Composite-hydroxide-mediated approach an effective synthesis route for BaTiO 3 functional nanomaterials. Appl Phys A. 2016;122(4):2016. doi: 10.1007/s00339-016-9766-7.
13. Sundharam E, Jeevaraj AKS, Chinnusamy C. Effect of ultrasonication on the synthesis of barium oxide nanoparticles. J Bionanosci. 2017;11(4):310-4. doi: 10.1166/jbns.2017.1449.
14. Verma DK, Patel S, Kushwah KS. Synthesis of titanium dioxide (TiO_2) nanoparticles and impact on morphological changes, seeds yield and phytotoxicity of *Phaseolus vulgaris* L. Trop Plant Res. 2020;7(1):158-70. doi: 10.22271/tpr.2020.v7.i1.021.
15. Vanaja M, Annadurai G. *Coleus aromaticus* leaf extract mediated synthesis of silver nanoparticles and its bactericidal activity. Appl Nanosci. 2013;3(3):217-23. doi: 10.1007/s13204-012-0121-9.
16. Choudhury R, Majumder M, Roy DN, Basumallick S, Misra TK. Phytotoxicity of Ag nanoparticles prepared by biogenic and chemical methods. Int Nano Lett. 2016;6(3):153-9. doi: 10.1007/s40089-016-0181-z.
17. Darwish AGA, Badr Y, El Shaarawy M, Shash NMH, Battisha IK. Influence of the Nd3+ ions content on the FTIR and the visible up-conversion luminescence properties of nano-structure BaTiO3, prepared by sol–gel technique. J Alloys Compd. 2010;489(2):451-5. doi: 10.1016/j.jallcom.2009.09.021.
18. Phan TTM, Chu NC, Luu VB, Nguyen Xuan H, Pham DT, Martin I, *et al*. Enhancement of polarization property of silane-modified BaTiO3 nanoparticles and its effect in increasing dielectric property of epoxy/BaTiO3 nanocomposites. J Sci Adv Mater Devices. 2016;1(1):90-7. doi: 10.1016/j.jsamd.2016.04.005.
19. Saleem S, Muhammad G, Hussain MA, Altaf M, Bukhari SNA. *Withania somnifera* L.: insights into the phytochemical profile, therapeutic potential, clinical trials, and future prospective. Iran J Basic Med Sci. 2020;23(12):1501-26. doi: 10.22038/IJBMS.2020.44254.10378, PMID 33489024.
20. Azam A, Ahmed AS, Ansari MS, Shafeeq M MM, Naqvi AH. Study of electrical properties of nickel doped SnO2 ceramic nanoparticles. J Alloys Compd. 2010;506(1):237-42. doi: 10.1016/j.jallcom.2010.06.184.
21. Khan MAM, Kumar S, Ahamed M, Ahmed J, Kumar A, Shar MA. BaTiO3@rGO nanocomposite: enhanced photocatalytic activity as well as improved electrode performance. J Mater Sci Mater Electron. 2021;32(10):12911-21. doi: 10.1007/s10854-020-04514-0.
22. Khan MAM, Kumar S, Ahmed J, Ahamed M, Kumar A. Influence of silver doping on the structure, optical and photocatalytic properties of Ag-doped BaTiO3 ceramics. Mater Chem Phys 2021;259:124058. 2021;259. doi: 10.1016/j.matchemphys.2020.124058.
23. Haroon A, Rai P, Uddin I. Synthesis, characterization and dielectric properties of BaTiO3 nanoparticles. Int J Nanosci. 2020;19(1). doi: 10.1142/S0219581X19500017.

Cite this article: Palusamy R, Ganesan T, Appakan S, Chandrasekaran T, Sangilimuthu Ay, Structural, Optical, Antibacterial and Anticancer Properties Silver Barium Modified Titanium Dioxide Nanoparticles Prepared via a Green Process Using *Withania somnifera* Hairy Roots. Asian J Biol Life Sci. 2023;12(2):294-300.